



COMPOSITE MASS DAMPERS FOR VIBRATION CONTROL OF WIND-EXCITED TOWERS

N. YAN, C. M. WANG AND T. BALENDRA

*Department of Civil Engineering, The National University of Singapore,
10 Kent Ridge Crescent, 119260 Singapore*

(Received 26 March 1997, and in final form 30 December 1997)

Various systems for controlling the vibrations of tall buildings subjected to earthquakes or strong winds have been developed and applied over the past few years. This paper is concerned with the use of a composite active-passive tuned mass damper (APTMD) system for the vibration control of a single-degree-of-freedom tower under the along-wind and the across-wind excitations, respectively. The effectiveness of this relatively new composite tuned mass damper system is investigated and compared with the more well-known active tuned mass damper system. The results show reductions in the wind-induced displacement responses of the towers are greater with APTMD if the appropriate damper and control parameters are selected. More importantly, these better performances may be achieved with a relatively smaller mass for the active part of the control. Such a smaller active damper mass is advantageous for installation purposes. The parametric studies conducted herein also show that the APTMD system is not so sensitive to the small variations of the structure-damper mass ratio, the frequency ratio and damping factor of the damper. These APTMD characteristics are useful in design.

© 1998 Academic Press Limited

1. INTRODUCTION

Modern buildings and towers tend to be lighter, more slender and possess smaller natural damping when compared to their older counterparts. These structures are thus more prone to excessive wind and earthquake induced oscillations. One way to mitigate the vibrations is to install damping systems. The most common damping device is the passive tuned mass damper (PTMD) which consists of an auxiliary mass in tune with the natural period of the buildings. Xu *et al.* [1] designed and tested a 1:400 scale aeroelastic model of the CAARC Standard Tall Building with such a PTMD system in a wind tunnel. The test demonstrated the effectiveness of the tuned mass damper system in suppressing the dynamic response of the building. A comprehensive list of structures installed with such dampers has been compiled by Holmes [2]. Some examples of these structures are the John Hancock Building (Boston), the City Corp Centre (New York) and the Sydney Tower (Sydney). However, Fukushima *et al.* [3] pointed out that the passive tuned mass dampers have the following problems:

The tight restriction on the size of PTMD limits the control effect;

PTMD frequency cannot be readily adjusted when its frequency is out of tune with the structural frequency and thus leads to a significant drop in its effectiveness in vibration control.

To overcome the aforementioned setbacks of the PTMD, the active tuned mass damper (ATMD) device has been developed. This device requires a control algorithm that analyses the dynamic structural feedbacks to create a control force that drives a mass. Extensive investigations on the active control system covering both the theoretical and the experimental aspects have shown that structural vibrations can be further reduced using such a control system over the passive control system. For example, Roorda [4] found that a more effective attenuation of the vibration responses of tall flexible structures could be achieved in the first mode by a feedback control. Nishimura *et al.* [5] developed a simplified algorithm to optimise the feedback gains and the damper parameters for efficient control performance of ATMD. Based on experimental and theoretical studies, Kwok and Samali [6] found that the effectiveness of PTMD in suppressing wind-induced tall building motion could be enhanced by the addition of an active control capacity. Suhardjo *et al.* [7] proposed a frequency domain approach to optimal control of wind-excited buildings in which the H_2 norm of the transfer function from the external disturbance to the regulated output is minimised. To illustrate the methodology, a 60-storey building under an along-wind excitation was employed to show reduction in the acceleration response of the building. Xu [8] set up a method for selecting design parameters of the active mass dampers and estimating motion reduction of wind-excited tall building, based on a aeroelastic model test of uncontrolled tall building. His findings showed that the wind-induced responses of the plain buildings (i.e., without any control device) could be substantially reduced if acceleration sensors were used and the parameters of the active mass damper were selected appropriately.

Recently, Nishimura *et al.* [9] proposed that an active TMD be attached to a passive TMD. They claimed that such a hybrid active-passive mass damper system (APTMD) has the following advantageous features:

Compared with other conventional ATMD system, the size of the active controller is significantly smaller which is an advantage when installed in structures;

The required control force or power for activating the device is significantly smaller as compared with the expected vibration control performance;

The passive TMD works as a mechanical filter to cut off the high frequency noise vibration of the active mechanism from reaching the structure.

Based on the vibration analysis of a single-degree-of-freedom structure under harmonic excitation, Nishimura *et al.* [9, 10] and Fukushima *et al.* [3] showed that the composite APTMD system can produce a large improvement in the control performance over the PTMD system.

The purpose of this investigation is to study the effectiveness of APTMD in vibration control of towers under along-wind and across-wind excitation spectra described by an appropriate method. As in reference [8], displacement, velocity and acceleration sensors are first conducted to establish the most appropriate sensor for the effectiveness of APTMD. Secondly, the influence of structural characteristics on frequency response function of structure is considered to minimise the input of external energy into the structure. In addition, parametric studies are conducted on the control parameters with the view to obtain some design guidelines for such a composite tuned mass damper system.

2. GOVERNING EQUATIONS FOR COMPOSITE MASS DAMPER SYSTEM

Consider a tower modelled as a single-degree-of-freedom structure subjected to wind force $f(t)$. The structural displacement $x_s(t)$ is to be damped using the composite

active-passive tuned mass dampers (APTMD) as shown in Figure 1. The equations of the composite mass damper system are given by (Nishimura *et al.* [9])

$$M_S \ddot{x}_S + C_S \dot{x}_S + K_S x_S - C_P \dot{x}_P - K_P x_P = f(t), \tag{1}$$

$$M_P (\ddot{x}_S + \ddot{x}_P) + C_P \dot{x}_P + K_P x_P - C_A \dot{x}_A - K_A x_A + u(t) = 0, \tag{2}$$

$$M_A (\ddot{x}_S + \ddot{x}_P + \ddot{x}_A) + C_A \dot{x}_A + K_A x_A - u(t) = 0, \tag{3}$$

where M_S , M_P and M_A are mass of the tower, the passive TMD and the active TMD, respectively; K_S , K_P and K_A are stiffness of the tower, the passive TMD and the active TMD respectively; C_S , C_P and C_A are the damping of the tower, the passive TMD and the active TMD respectively; x_S is the displacement response of the tower; x_P , x_A are the relative displacement responses of the passive TMD and the active TMD respectively; $f(t)$ is the wind force; $u(t)$ is the control force and the superdot denotes differentiation with respect to time.

For analysis, the frequency domain approach will be adopted since the dynamic behaviour of a structure can often be described more simply by the transfer function in the frequency domain, and the excitations on a structure, such as wind loads, are often modelled as stochastic processes characterised by their spectral density functions in the frequency domain. Adopting this approach, (1)–(3) may be cast into

$$\begin{Bmatrix} x_S(t) \\ x_P(t) \\ x_A(t) \\ u(t) \\ f(t) \end{Bmatrix} = \begin{Bmatrix} X_S(\omega) \\ X_P(\omega) \\ X_A(\omega) \\ U(\omega) \\ F_0 \end{Bmatrix} e^{i\omega t}, \tag{4}$$

where $X_S(\omega)$, $X_P(\omega)$, $X_A(\omega)$ and $U(\omega)$ are the Fourier transforms of $x_S(t)$, $x_P(t)$, $x_A(t)$ and $u(t)$, respectively; ω is the frequency of the wind excitation and F_0 the wind force.

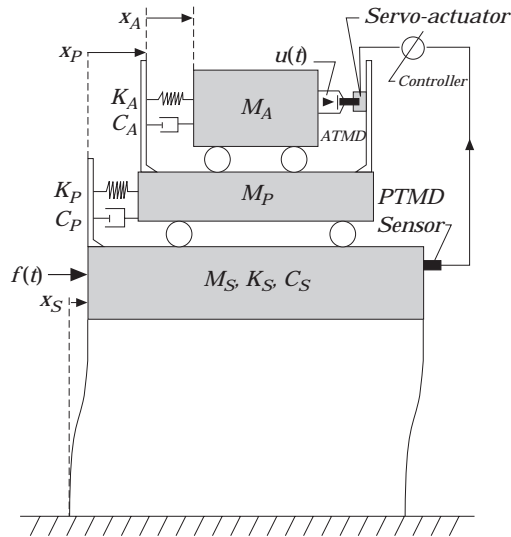


Figure 1. Composite active-passive tuned mass damper (APTMD) system fitted on a single-degree-of-freedom tower.

TABLE 1
Expressions of g_1 and g_2 for different sensors

Type of Sensors	g_1	g_2
Displacement sensor	$(K_i/K_S)(\tau\epsilon^2/[\epsilon^2 + \beta^2])$	$-(K_i/K_S)(\tau\epsilon/([\epsilon^2 + \beta^2]))$
Velocity sensor	$(K_i/K_S)\tau\epsilon\beta^2/[\epsilon^2 + \beta^2]$	$(K_i/K_S)\tau\epsilon^2/([\epsilon^2 + \beta^2])$
Acceleration sensor	$-(K_i/K_S)\tau\epsilon^2\beta^2/([\epsilon^2 + \beta^2])$	$(K_i/K_S)\tau\epsilon\beta^2/([\epsilon^2 + \beta^2])$

Roorda [4] has established the following relationship between the control force $U(\omega)$ and the controlled tip displacement of tower $X_S(\omega)$

$$U(\omega) = K_i(i\beta)^r \frac{\tau\epsilon}{\epsilon + i\beta} X_S(\omega), \quad (5)$$

where

$r = 0$ for the displacement type sensor; 1 for the velocity type sensor; 2 for the acceleration type sensor.

$$\beta = n/n_s, \quad \epsilon = R_1/2\pi n_s, \quad \tau = (2\pi n_0)^r S_0/R_0. \quad (6a-c)$$

In (5), the parameter K_i represents a proportionality constant between the control force and the movement of the hydraulic piston; the parameter ϵ and τ are the normalised loop gain and feedback gain respectively; β is the normalised excitation frequency; n the wind excitation frequency; n_s the frequency of the tower; $1/R_0$ the feedback gain of the transducer in the servomechanism; R_1 the collective loop gain of the electrohydraulic servomechanism and S_0 the proportional constant between the sensed structural response and the output voltage from the sensor.

In view of (4)–(6), equations (1)–(3) may be expressed as

$$\begin{bmatrix} h_{11} & h_{12} & h_{13} \\ h_{21} & h_{22} & h_{23} \\ h_{31} & h_{32} & h_{33} \end{bmatrix} \begin{Bmatrix} X_S(\omega) \\ X_P(\omega) \\ X_A(\omega) \end{Bmatrix} = \begin{Bmatrix} F \\ 0 \\ 0 \end{Bmatrix}, \quad (7)$$

where

$$h_{11} = 1 - \beta^2 + 2\zeta_S(i\beta), \quad h_{12} = -\mu_P\Omega_P^2 - 2\mu_P\Omega_P\zeta_P(i\beta), \quad h_{13} = 0 \quad (8a-c)$$

$$h_{21} = g_1 - \beta^2\mu_P + g_2(i\beta), \quad h_{22} = (\Omega_P^2 - \beta^2)\mu_P + 2\mu_P\Omega_P\zeta_P(i\beta), \quad (8d, e)$$

$$h_{23} = -\mu_A\Omega_A^2 - 2\mu_A\Omega_A\zeta_A(i\beta), \quad h_{31} = -g_1 - \beta^2\mu_A - g_2(i\beta), \quad h_{32} = -\beta^2\mu_A, \quad (8f, h)$$

$$h_{33} = (\Omega_A^2 - \beta^2)\mu_A + 2\mu_A\Omega_A\zeta_A(i\beta), \quad (8i)$$

$$\mu_P = M_P/M_S, \quad \mu_A = M_A/M_S, \quad \Omega_P = \omega_P/\omega_S, \quad \Omega_A = \omega_A/\omega_S,$$

$$\zeta_S = C_S/2M_S\omega_S, \quad \zeta_P = C_P/2M_P\omega_P, \quad \zeta_A = C_A/2M_A\omega_A, \quad F = F_0/M_S\omega_S^2 \quad (9a-h)$$

and the expressions of g_1 and g_2 are given in Table 1.

By solving (7), one obtains the following transfer functions

$$H_S(i\beta) = X_S(\omega)/F = \frac{\chi_1}{\chi_2}, \quad H_P(i\beta) = X_P(\omega)/F = 1/h_{12} - (h_{11}/h_{12})(\chi_1/\chi_2), \quad (10, 11)$$

$$H_A(i\beta) = X_A/F = -h_{22}/h_{12}h_{23} + (h_{11}h_{22}/h_{12}h_{23} - h_{21}/h_{23})\chi_1/\chi_2. \quad (12)$$

TABLE 2(a)
Properties of towers considered

Tower Parameter	Tower A	Tower B	Tower C
Height H (m)	80	186	250
Mass M_S (kg)	6.54×10^6	1.52×10^7	2.05×10^7
Frequency ω_S (rad/s)	2.922	1.256	0.935

TABLE 2(b)
Mass damper parameters

	Passive TMD	Active TMD
Mass ratio (μ)	$0.04(1-\alpha)$	0.04α
Frequency ratio (Ω)	0.97	0.97
Damping factor (ζ)	0.0975	0.0975

Note: α is mass ratio between the active tuned mass damper and the total mass dampers.

TABLE 3
Values for wind parameters

Wind parameters	Values for wind property	Wind parameters	Values for wind property
k_0	0.03	σ_L	0.6
l_x (m)	1200	A	2.0
U_{10} (m/s)	20	A_C	1.26
ρ_0 (kg/m ³)	1.2	S	0.11
C_0	1.2	—	—

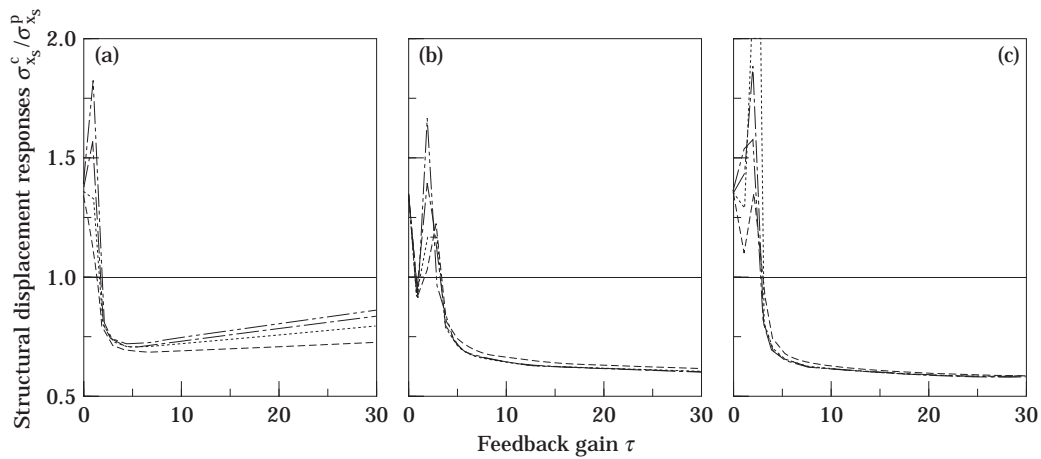


Figure 2. Effect of different types of sensor on the normalised structural displacements. (a) Displacement, (b) velocity and (c) acceleration sensors. Key: ϵ values ----, 2; ····, 5; - · - ·, 10; - - - - - , 20.

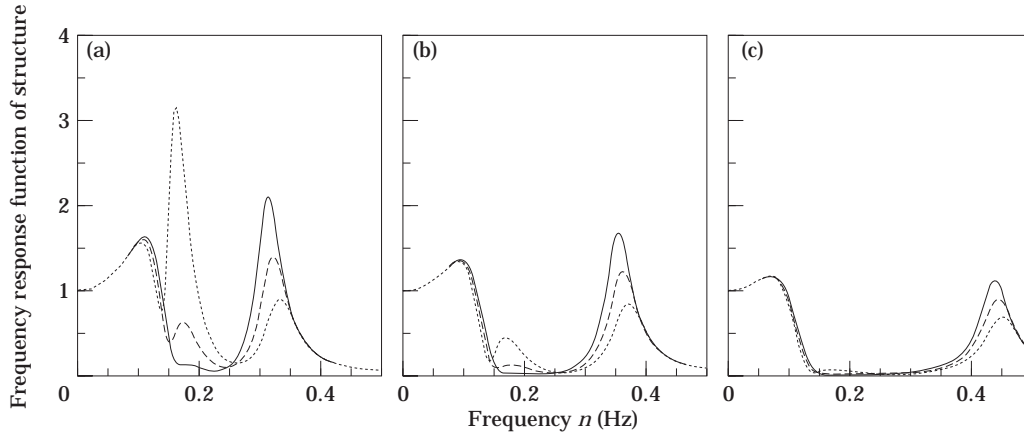


Figure 3. Influence of damper mass ratio on structural frequency response function when feedback gain is set to be (a) $\tau = 10$, (b) $\tau = 20$, and (c) $\tau = 50$. Key: α values —, 0.1; ----, 0.2; ·····, 0.3.

where

$$\chi_1 = (h_{23}h_{32} - h_{22}h_{33})/h_{12}, \quad \chi_2 = h_{21}h_{33} - h_{23}h_{31} + h_{11}(h_{23}h_{32} - h_{22}h_{33})/h_{12}. \quad (13a, b)$$

The power spectra of the displacement responses of the tower, the PTMD and the ATMD can be, respectively, expressed as

$$S_{x_S}^c = |H_S(i\beta)|^2 S_{FF}(\beta), \quad S_{x_P}^c = |H_P(i\beta)|^2 S_{FF}(\beta), \quad S_{x_A}^c = |H_A(i\beta)|^2 S_{FF}(\beta), \quad (14-16)$$

where $S_{FF}(\beta)$ is the non-dimensional power spectral densities of the along-wind force or across-wind force.

For the along-wind, the two-sided Harris spectrum is adopted. This non-dimensional power spectral density is given by Balendra *et al.* [11] as

$$S_{FF}(\beta) = (4k_0 \bar{F}^2 / \beta) \phi \quad (17)$$

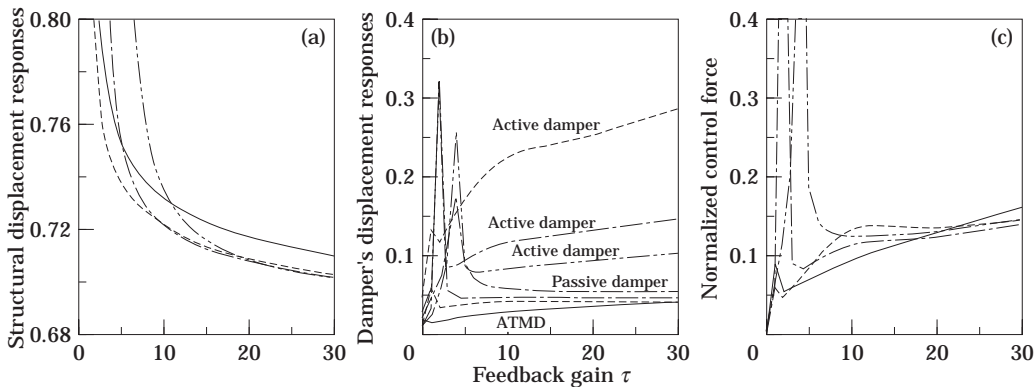


Figure 4. Variations of normalised structural displacement, damper displacement and control force against feedback gain for Tower A under along-wind excitation ($H = 80$ m, $\epsilon = 5$, $K_t/K_s = 0.05$). Key for α values —, 1; ----, 0.1; ·····, 0.2; -·-·-·, 0.3.

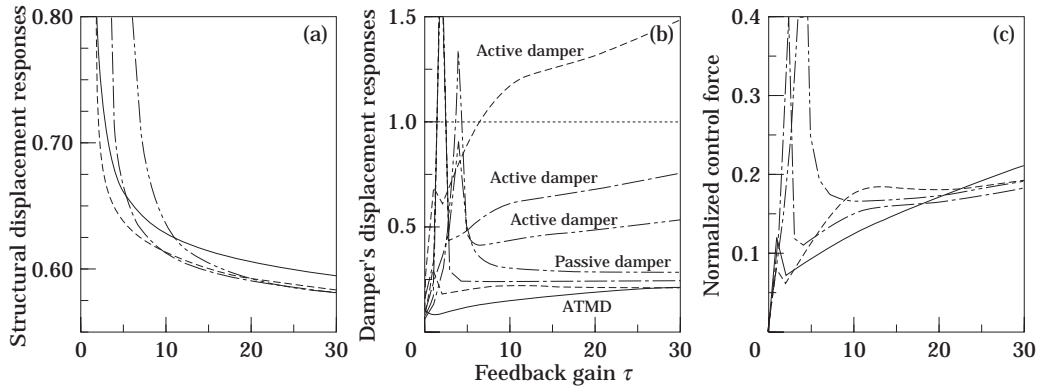


Figure 5. Variations of normalised structural displacement, damper displacement and control force against feedback gain for Tower B under along-wind excitation ($H = 186$ m, $\epsilon = 5$, $K_r/K_s = 0.05$). Key as for Figure 4.

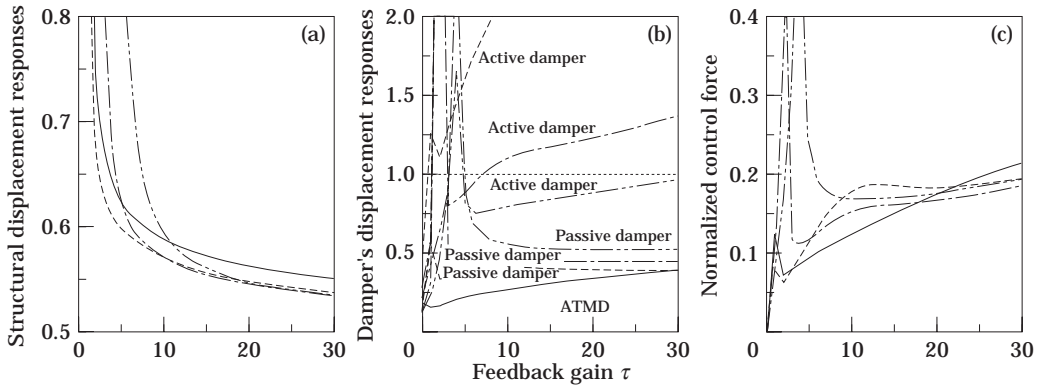


Figure 6. Variations of normalised structural displacement, damper displacement and control force against feedback gain for Tower C under along-wind excitation ($H = 250$ m, $\epsilon = 5$, $K_r/K_s = 0.05$). Key as for Figure 4.

where

$$\phi = \bar{U}_r^2 \pi^4 \psi \beta / [2 + (\pi^3 \psi \beta)^2]^{5/6}, \quad \bar{U}_r = U_{10}/U_z, \quad U_z = U_{10} \left(\frac{z}{10} \right)^{0.3},$$

$$\psi = \omega_s l_x / 2\pi^4 U_{10}, \quad \bar{F} = F_0 \pi^4 / \omega_s^2 M_s z, \quad F_0 = \rho_0 A_0 C_0 U_z^2, \quad (18a-f)$$

TABLE 4

Minimum values of τ and α for APTMD to be better than ATMD under along-wind

Tower	$\sigma_{x_s}^c < \sigma_{x_s}^a$		$\sigma_{x_D}^c < \sigma_m$		$\sigma_u^c < \sigma_u^a$		Recommended values		Damper disp for recommended values (m)	
	τ	α	τ	α	τ	α	τ	α	σ_{xp}	σ_{xA}
A	≥ 11	≥ 0.1	≥ 5	≥ 0.1	≥ 20	≥ 0.1	20	0.1	0.04	0.25
B	≥ 11	≥ 0.1	≥ 7	≥ 0.2	≥ 20	≥ 0.1	20	0.2	0.25	0.70
C	≥ 11	≥ 0.1	≥ 8	≥ 0.3	≥ 20	≥ 0.1	20	0.3	0.52	0.82

TABLE 5

Values of τ and α for APTMD to be better than ATMD under across-wind

Tower	$\sigma_{x_s}^c < \sigma_{x_s}^a$		$\sigma_{x_D}^c < \sigma_m$		$\sigma_u^c < \sigma_u^a$		Recommended values		Damper disp. for recommended values (m)	
	τ	α	τ	α	τ	α	τ	α	σ_{xp}	σ_{xu}
A	≥ 8	≥ 0.1	≥ 5	≥ 0.1	≥ 12	≥ 0.1	12	0.1	0.04	0.32
B	≥ 8	≥ 0.1	5–22	≥ 0.2	≥ 12	≥ 0.2	12	0.2	0.20	0.71
C	≥ 8	≥ 0.1	5–20	≥ 0.3	≥ 12	≥ 0.2	12	0.3	0.50	0.75

in which k_0 is the ground surface drag coefficient, l_x the wave length, z the height of tower, ω_s the circular frequency of tower, U_{10} the mean wind speed at the reference height of 10 m. ρ_0 density of air; A_0 the frontal area of tower; C_0 the drag coefficient, and U_z the mean wind speed at the height z .

For the across-wind, a new empirical formula for the across-wind spectra proposed by Choi and Kanda [12] is adopted for the present study. The spectral form can be decomposed into two parts, namely a narrow spectral peak due to the regular vortex shedding and a wideband spectral distribution caused by vorticity in the separated shear layer and the shear layer-trailing edge direct interaction. The non-dimensional spectra of the across-wind force can be written as follows:

$$S_{FF}(\beta) = \frac{\bar{F}_y^2 \sigma_L^2}{\beta} B_1 A_C \frac{(\tilde{f}/k)}{[1 + (\tilde{f}/k)^A]^{5/A}} + \frac{(1 - B_1)}{\sqrt{2\pi}\delta} \exp\left[-\frac{1}{2}\left(\frac{\ln \tilde{f} + 0.56\delta^2}{\delta}\right)^2\right], \quad (19)$$

where

$$\begin{aligned} A_C &= A\Gamma(5.0/A)/\Gamma(4.0/A)\Gamma(1.0/A), \\ B_1 &= \sqrt{I_u(z/3)}\{1 + (3D/5B)^6\}^{0.8} \quad \text{for } D/B \leq 3.0, \\ k &= 1.58\sqrt{B/D}, \quad \delta = I_u(z/3) \quad \text{for } D/B < 1.0, \\ k &= 1.58, \quad \delta = 1.58\sqrt{D/BI_u(z/3)} \quad \text{for } D/B \geq 1.0, \\ \bar{F}_y &= \rho_0 A_0 U_z^2 / 2M_S \omega_s^2 z, \quad \tilde{f}_s = n/f_s, \quad f_s = SU_z/B. \end{aligned} \quad (20a-i)$$

In Equations (19) and (20), σ_L represents the standard deviation of lift coefficient; $\Gamma(\cdot)$ the gamma function; f_s the vortex shedding; S the Strouhal number; I_u the turbulence intensity and B and D are the breadth and depth of the tower respectively. The parameter A affects the energy distribution on the lower frequency range. In this study, A is assumed to be 2.0. The value of A_C becomes 1.26.

For the purpose of quantifying the dynamic responses of the tower with and without a damper system, the following normalised standard deviations of the displacement responses are introduced:

For structural displacement response

$$\sigma_{x_s}^i / \sigma_{x_s}^o = \left[\int_0^\infty S_{x_s}^i(\beta) d\beta \right]^{1/2} / \left[\int_0^\infty S_{x_s}^o(\beta) d\beta \right]^{1/2}, \quad (21)$$

For damper displacement response

$$\sigma_{x_D}^i / \sigma_{x_S}^o = \left[\int_0^\infty S_{x_D}^i(\beta) d\beta \right]^{1/2} / \left[\int_0^\infty S_{x_S}^o(\beta) d\beta \right]^{1/2}, \quad (22)$$

where the superscript i takes on different letters as: $i = c$ for tower with composite APTMD system; a for tower with ATMD system; p for tower with PTMD system; o for tower without any control system and the subscript D denotes the type of dampers, i.e., $D = A$ for the active TMD; P for the passive TMD.

It is clear that the foregoing ratios will always be less than unity. The smaller the values of these ratios, the more effective is the vibration control of the damper system.

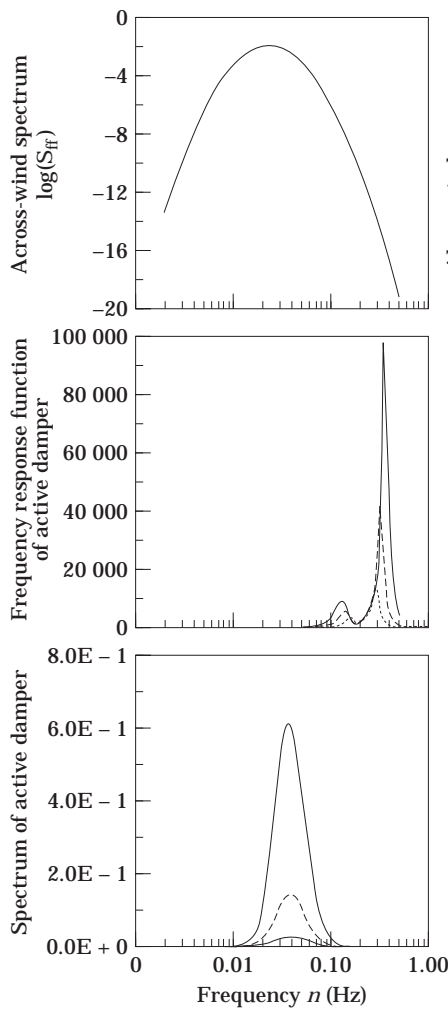


Figure 7. Frequency response function and spectrum of active damper under across-wind excitation. Key for τ values: —, 25; ----, 12; , 5.

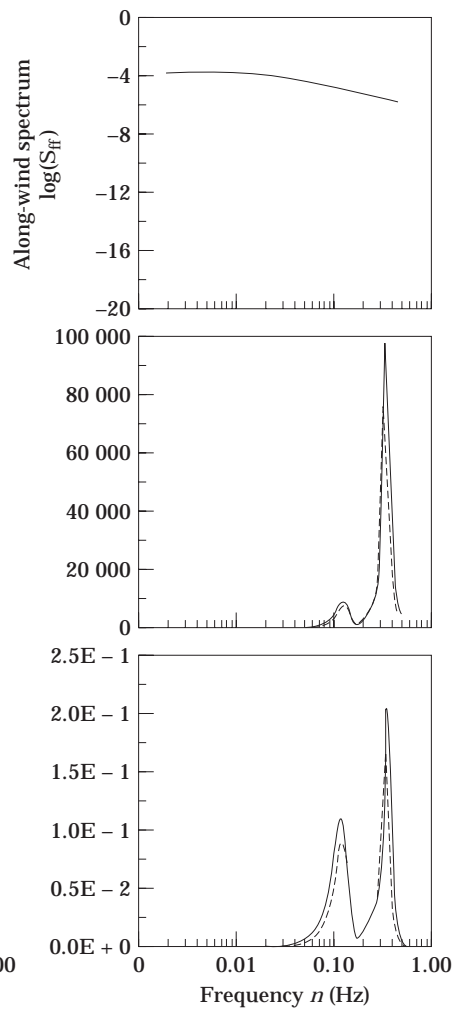


Figure 8. Frequency response function and spectrum of active damper under along-wind excitation. Key for τ values: —, 25; ----, 20; , 5.

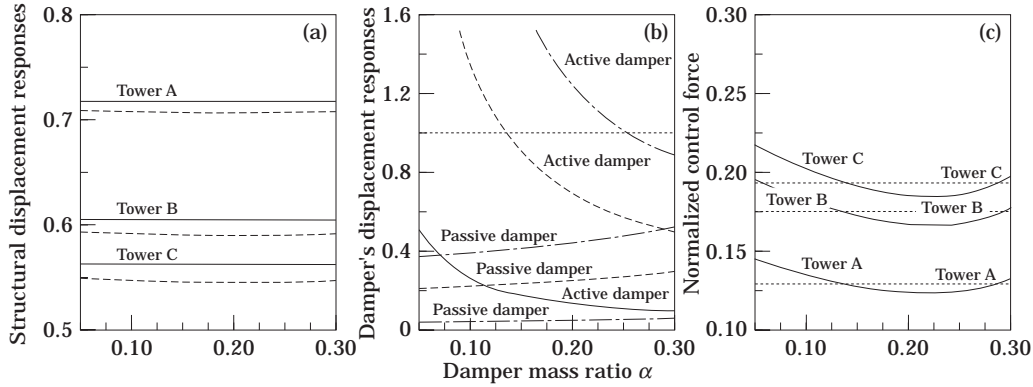


Figure 9. Variations of normalised structural displacement, damper displacement and control force against damper mass ratio for feedback gain $\tau = 20$ under along-wind excitation. (a) —, with ATMD; ----, with APTDM. (b) —, Tower A, ----, Tower B; -·-·-, Tower C. (c) ····, with ATMD; —, with APTMD.

To ascertain the level of control force required to reduce tower motion to a particular level when designing the damper system, the normalised standard deviation of the control force is introduced (Xu [8])

$$\sigma_u/\sigma_F = \left[\int_0^\infty \left| K_t(i\beta)^r \frac{\tau\epsilon}{\epsilon + i\beta} \right|^2 S_{x_s}^i(\beta) d\beta \right]^{1/2} / \left[\int_0^\infty S_{FF}(\beta) d\beta \right]^{1/2}. \quad (23)$$

The foregoing integrals have upper limits of infinity. However, for calculation purposes, this upper limit is taken as a finite value given by $\beta_{max} = n_{mas}/n_s$ where n_{mas} is the frequency at which the structural response spectra value is almost close to zero and n_s is the natural frequency of the structure.

3. EFFECTIVENESS OF COMPOSITE MASS DAMPERS

Xu [8] studied the use of an active mass damper in suppressing the motion of wind-excited tall buildings. He first investigated the effects of using different types of

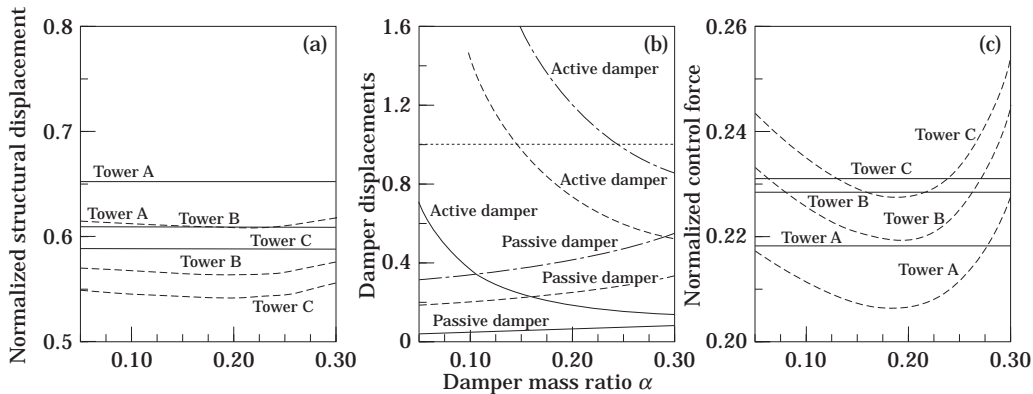


Figure 10. Variations of normalised structural displacement, damper displacement and control force against damper mass ratio for feedback gain $\tau = 12$ under across-wind excitation. (a) —, with ATMD; ----, with APTDM. (b) —, Tower A, ----, Tower B; -·-·-, Tower C. (c) —, ATMD; ---- with APTDM.

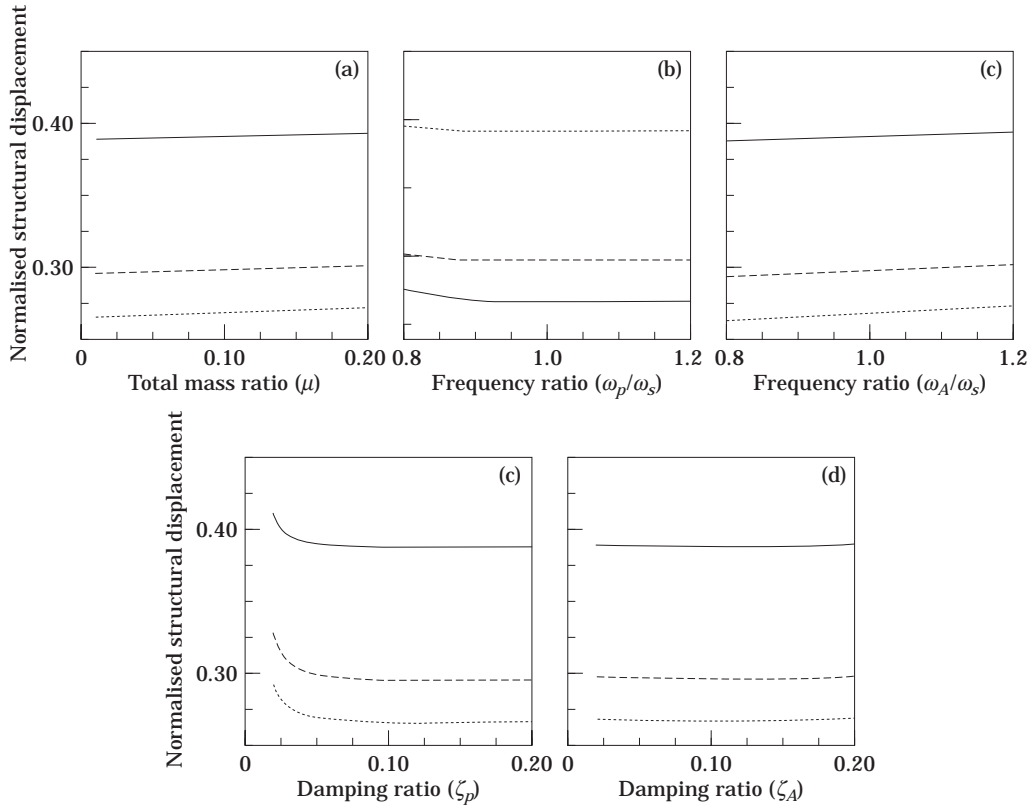


Figure 11. Effect of (a) mass ratio μ , (b) frequency with ω_p/ω_s , (c) frequency ratio ω_A/ω_s , (d) damper damping ζ_p and (e) damper damping ζ_A on the normalised structural displacement under along-wind excitation. Key: —, Tower A; ---, Tower B;, Tower C.

sensors and found that the acceleration sensor gave the largest building motion reduction for a large feasible design region of control parameters ϵ , τ . Based on extensive parametric studies, the appropriate values of parameters K_r , ϵ and τ were established for minimising the building responses and control forces. The values found $K_r/K_s = 0.05-10$, $\epsilon = 5-10$ and $\tau \geq 5$. The influences of structure-damper mass ratio, the frequency ratio and the damping factor of the damper were also examined. Here, Xu found that the active control system is rather insensitive to small variations of mass ratios, frequency ratios and damper damping factors.

Following along the line of Xu's work, this paper studies the same design considerations for the situation in which the active damper is to be used in conjunction with a passive damper. Empirical formulae for the spectra of the along-wind and the across-wind force are directly used for the external excitation. The effectiveness of the composite damper control system is determined by comparing its performance with a non-composite damper system. For the subsequent parametric studies, three towers representing short to tall towers are considered. This properties are given in Table 2a. The towers are fitted with a composite tuned mass damper system characterised by the parameter values given in Table 2b. For all computations, $K_r/K_s = 0.05$ has been adopted. Table 3 presents the adopted values for the wind parameters.

3.1. EFFECTS OF SENSOR TYPES

The normalised standard deviations of displacement response to Tower B with the composite APTMD are computed for different loop and feedback gain values, ϵ and τ under the along-wind excitation. A mass ratio between the active tuned mass damper and the total mass of the dampers of $\alpha = 0.2$ has been assumed for the composite damper system. Figures 2a–c show respectively the effects of using the displacement sensor, velocity sensor and acceleration sensor (for the active part of the control system) on the variations of the standard deviations of structural displacement responses $\sigma_{x_s}^c/\sigma_{x_s}^p$ with respect to the feedback gain τ for various feedback loop values ϵ . It can be seen that for the displacement sensor given in Fig. 2a, the structural displacement response $\sigma_{x_s}^c/\sigma_{x_s}^p$ is less than 1 when $\tau > 2$. This means that the composite TMDs system causes greater reduction than the passive system. And the reduction in the structural displacement decreases as the control parameter τ increases from 2 to 30. However, Figs. 2b and 2c indicate that the control effect of using the velocity sensor or acceleration sensor is obviously better than that of using the displacement sensor. The numerical data shows that the acceleration sensor yields the smallest response to the along-wind excitation. The same observations are made with the cases of Towers A and C but the results have not been presented as they are similar in nature to those given in Figure 2. The foregoing conclusion on the most effective sensor type for the composite damper system concurs with that stated by Xu [8] who studied a purely active damper control system.

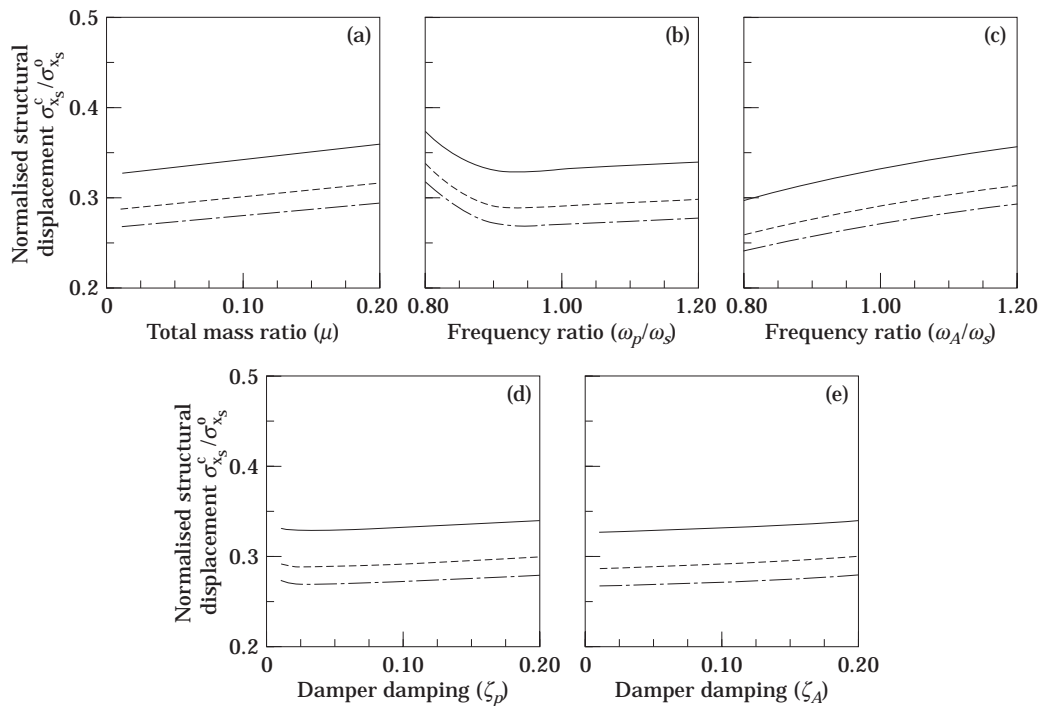


Figure 12. Effect of (a) mass ratio μ , (b) frequency with ω_p/ω_s , (c) frequency ratio ω_A/ω_s , (d) damper damping ζ_p and (e) damper damping ζ_A on the normalised structural displacement under across-wind excitation. Key as for Figure 11.

3.2. INFLUENCES OF τ AND α ON FREQUENCY RESPONSE OF STRUCTURE

The frequency response function of a structure represents its capacity of transferring external excitation energy to the structure itself. Its magnitude is dependent on the structural characteristics of the system. In order to minimise the input of external energy into the structure, the ordinates of the structural frequency response function should be small in the frequency range where external energy is large. Figs. 3(a), (b) and (c) illustrate the influence of damper mass ratio α on the frequency response of Tower B when an acceleration sensor is used with feedback gain $\tau = 10, 20$ and 50 respectively. It is seen from Fig. 3(a) that for $\tau = 10$, a smaller damper mass ratio is required to avoid large values of frequency response function, i.e., the mass of active damper should not exceed 20% of total damper mass for $\tau = 10$. Fig. 3(c) indicates that the influence of α on the frequency response function becomes less sensitive when $\tau = 50$. By comparing Figs. 3(a), 3(b) and 3(c), it is also seen that a larger feedback gain results in greater reduction in structural frequency response. From the above observations, it is evident that once the feedback gain is selected the damper mass ratio must be determined appropriately to ensure that less external energy transfers to the structure.

3.3. PERFORMANCE OF APTMD AS COMPARED TO ATMD

To study the effectiveness of the present composite APTMD over the ATMD, the three towers were analysed under the along-wind and the across-wind excitations, with different damper mass ratios $\alpha = 0.1, 0.2, 0.3$ and 1.0 . The acceleration sensor was used with $K_t/K_s = 0.05$ and loop gain $\epsilon = 5$.

Figures 4–6 show the structural displacement, damper displacements and the control force for the three towers, normalised respectively by the structural displacement of the PTMD system, maximum permissible damper movement (taken to be 1 m, Kwok *et al.* [6]) and wind force. It is seen from Figures 4a, 5a and 6a that the composite APTMD performs better than the ATMD ($\alpha = 1$) when an appropriate feedback gain is chosen. However, it is evident from Figures 4b, 5b and 6b that the damper motions for APTMD is larger than that of ATMD. Nevertheless, by choosing an appropriate damper mass ratio and feedback gain, it is possible to maintain the movement of the damper within the permissible range. From Figures 4c, 5c and 6c, it can be seen that the control force required in the APTMD system under the along-wind excitation is less than that of the ATMD when the feedback gain $\tau > 20$.

Table 4 summarises the range of τ and α for APTMD to be better than ATMD under along-wind excitation. The recommended values for each tower given in the same table indicate that larger damper mass is required for taller structures. The displacements of both passive and active dampers for the recommended values of τ and α are well within the allowable limit as indicated in this Table. The corresponding results for the across-wind excitation are presented in Table 5. It is to be noted that unlike in the cases of along-wind, for the across-wind the feedback gain is bounded for Towers B and C. The lower limit τ is to ensure a stable system response whereas the upper limit restricts the motion of the active damper within permissible limit. For instance, in the case of Tower B, Figure 7 illustrates why the response of the active damper is quite large at $\tau = 25$ compared to $\tau = 12$ and $\tau = 5$ for across-wind excitation. The normalised variation of displacement of the active damper for $\tau = 25$ is 1.06 while 0.49 for $\tau = 12$ and 0.20 for $\tau = 5$. The corresponding curves with $\tau = 25$ and $\tau = 20$ are plotted in Figure 8 for along-wind. The related variation is 0.56 for $\tau = 25$ and 0.49 for $\tau = 20$.

The advantage of using the APTMD is that the active mass damper component may be of relatively smaller size when compared to that employed in a purely ATMD system.

A smaller active mass damper enables easy installation. In order to fine tune the recommended mass ratios given in Tables 4 and 5, Figure 9 and 10 are plotted for along and across wind excitation respectively.

Figures 9 and 10 present the normalised structural displacement, damper displacements and control force as the damper mass ratio α changes from 0.05 to 0.30. The feedback gain τ is set to be 20 for along-wind excitation and 12 for across-wind excitation. In Figures 9(a), (b) and (c), it is seen that under along-wind excitation the best damper mass ratio α should be 0.225 for Tower A, Tower B, and 0.26 for Tower C. When these damper mass ratios are adopted, the structural displacement with APTMD is less than that with ATMD; the control force is more or less the smallest; and the damper displacements are within the maximum permissible range. Similarly for across-wind, Figures 10(a), (b) and (c) show that the optimum damper mass ratios are 0.18 for Tower A, Tower B, and 0.25 for Tower C.

3.4. SENSITIVITY STUDY

The structural characteristics of a building or a tower, such as mass, stiffness and damping, cannot be determined accurately. In order to investigate the influences of the structural characteristics on the performance of APTMD, a sensitivity study of the normalised structural response to the total mass damper ratio μ , the frequency ratio Ω_p , Ω_A and the damping ratio ζ_p , ζ_A of dampers is conducted. The recommended values of τ and α in Tables 4 and 5 are used for each case. The results are shown in Figures 11a–11e for along-wind excitation and Figures 12a–12e for across-wind excitation. It is clear from Figures 11a–11e that the structural responses under the along-wind force are not sensitive to the total damper-structure mass ratio, damper-structure frequency ratios and damping ratios of the dampers. Also, Figure 12a–12e indicate that the normalised structural displacements are not affected by the total mass ratio, the damper-structure frequency ratios and the damping ratios of dampers within a considerable range. The performance of APTMD system, not being sensitive to the small variations of the structural characteristics, is very useful in practice.

4. CONCLUSIONS

The effectiveness of using composite active-passive tuned mass dampers for controlling vibration in towers due to random wind excitation has been studied. It is found that among displacement, velocity and acceleration sensors, the acceleration sensor is the most effective for obtaining the greatest reduction in structural displacement. The investigation on structural frequency response function shows that the system parameters must be selected appropriately to ensure that less external energy transfers to the structure. The study on the performance of APTMD indicates that such an APTMD further reduces the structural displacements when compared to its equivalent ATMD by using the appropriate feedback gain. Here the term “equivalent” implies that the total mass for the dampers in the APTMD is kept the same as the mass for the active damper in the ATMD. Although the damper displacements are larger in the APTMD system, they are still within permissible limit if feedback gain and damper mass ratio are chosen appropriately. The best values for feedback gain and damper mass ratio are given in this paper for different tower heights under along-wind and across wind excitation. It is found that larger damper mass ratio is needed to taller towers. The control force is somewhat the smallest when the optimum values of feedback gain and damper mass ratio are used. Through the sensitivity study, it is found that APTMD is not sensitive to the uncertainties of structure and damper, such as total mass ratio, frequency ratios and damping ratios of dampers.

A designer may opt for the composite APTMD system, because it requires a smaller active tuned mass damper size which is advantageous for installation purposes. The other practical advantage is that such composite active-passive mass damper system is not affected by the small variations of the structure-damper system.

ACKNOWLEDGMENT

The authors are very grateful to the reviewers for their comments and suggestions which have improved the quality of this work.

REFERENCES

1. Y. L. XU, K. C. S. KWOK and B. SAMALI 1992 *Journal of Wind Engineering and Industrial Aerodynamics* **40**, 1–32. Control of wind-induced tall building vibration by tuned mass dampers.
2. D. HOLMES 1995 *Engineering Structures* **17**, 676–677. Listing of installations.
3. I. FUKUSHIMA, K. SASAKI, T. NISHIMURA, N. KOSHIKA, M. SAKAMOTO and T. KOBORI 1995 *Proceedings of the Pacific Conference on Earthquake Engineering, Australia*, 267–276. Development and application of active-passive composite tuned mass damper to high-rise building.
4. J. ROORDA 1975 *American Society of Civil Engineers, Journal of the Structures Division* **101**(ST3), 505–521. Tendon control in tall structures.
5. I. NISHIMURA, T. KOBORI, M. SAKAMOTO, N. KOSHIKA, K. SASAKI and S. OHRUI 1992 *Proceedings of the First European Conference on Smart Structures and Materials, Glasgow*, 301–304. Acceleration feedback method applied to active tuned mass damper.
6. K. C. S. KWOK and B. SAMALI 1995 *Engineering Structures* **17**, 655–667. Performance of tuned mass dampers under wind loads.
7. J. SUHARDJO, B. F. SPENCER, JR. and A. KAREEM 1992 *Journal of Wind Engineering and Industrial Aerodynamics*, 41–44, 1985–1996. Active control of wind excited buildings: a frequency domain based design approach.
8. Y. L. XU 1996 *Journal of Engineering Structures* **18**, 64–76. Parametric study of active mass dampers for wind-excited tall buildings.
9. I. NISHIMURA, T. KOBORI, M. SAKAMOTO, T. YAMADA, N. KOSHIKA, K. SASAKI and S. OHRUI 1993 *Proceedings of the Seminar on Seismic Isolation, Passive Energy Dissipation and Active Control* **2**, ATC-17-1, 737–748. Active passive composite tuned mass damper.
10. I. NISHIMURA, M. SAKAMOTO, T. YAMADA, T. KOSHIKA and T. KOBORI 1994 *Journal of Structural Control* **1**, 103–116. Acceleration feedback method applied to active-passive composite tuned mass damper.
11. T. BALENDRA, C. M. WANG and H. F. CHEONG 1995 *Engineering Structures* **17**, 668–675. Effectiveness of tuned liquid column dampers for vibration control of towers.
12. H. CHOI and J. KANDA 1993 *Journal of Wind Engineering and Industrial Aerodynamics* **46** and **47**, 507–516. Proposed formulae for the power spectral densities of fluctuating lift and torque on rectangular 3-D cylinders.

APPENDIX: LIST OF NOTATION

A	parameter of affecting energy distribution on lower frequency range
A_0	frontal area of tower
B	breadth of tower
C_0	drag coefficient which is taken to be equal to 1.2
C_S, C_P, C_A	damping of tower, passive TMD and active TMD, respectively
D	depth of tower
$f(t)$	along-wind force
f_s	frequency of vortex shedding
$G(\omega)$	control gains in frequency domain
I_u	turbulence intensity
K_S, K_P, K_A	stiffness of tower, passive TMD and active TMD, respectively

K_f	proportional constant between the control force and the movement of the hydraulic piston
k_0	ground surface drag coefficient which is taken to be equal to 0.03
l_x	wave length which is taken to be equal to 1200 m
M_S, M_P, M_A	mass of tower, passive TMD and active TMD, respectively
n_S	frequency of tower
$1/R_0$	feedback gain of the transducer in the servomechanism
R_1	collective loop-gain of the electrohydraulic servomechanism
S	Strouhal number
S_0	proportional constant between the sensed structure response and the output voltage from the sensor
S_{FF}	power spectral density of wind force
$S_{x_S}^c, S_{x_P}^c, S_{x_A}^c$	power spectral density of tower, passive TMD and active TMD with composite control, respectively
$S_{x_S}^c$	power spectral density of tower without any control
X_S	displacement response of tower in frequency domain
x_S	displacement response of tower in time domain
X_P, X_A	relative displacement responses of passive TMD and active TMD in frequency domain, respectively
x_P, x_A	relative displacement responses of passive TMD and active TMD in time domain, respectively
U_{10}	mean wind speed at the reference height, 10 m
U_z	mean wind speed at height z
$U(\omega)$	control force in frequency domain
$u(t)$	control force in time domain
z	height of tower
α	damper mass ratio
β	normalised frequency ratio
ϵ	normalised loop gain
$\zeta_S, \zeta_P, \zeta_A$	damping factor of tower, passive TMD and active TMD, respectively
μ_P, μ_A	mass ratio of passive TMD and active TMD over tower, respectively
ρ_0	density of air which is taken to be equal to 1.2 kg/m ³
σ_F	standard deviation of along-wind force
σ_L	standard deviation of lift coefficient
σ_m	standard deviation of maximum permissible value of damper movement
$\sigma_{x_S}^o$	standard deviation of displacement response of tower without any control
$\sigma_{x_S}^c, \sigma_{x_P}^c, \sigma_{x_A}^c$	standard deviation of displacement response of tower, passive TMD and active TMD in composite APTMD system, respectively
$\sigma_{x_S}^p$	standard deviation of displacement response of tower with PTMD system
σ_u	standard deviation response of control force
τ	normalised feedback gain
Ω_P, Ω_A	frequency ratio of passive TMD and active TMD over tower, respectively
ω	circular frequency of along-wind excitation
$\omega_S, \omega_P, \omega_A$	circular frequency of tower, passive TMD and active TMD, respectively